

# Understanding the transition from Fraunhofer diffraction to the Geometrical Optics limit with single slits

Almudena García-Sánchez and Ángel S. Sanz

Department of Optics, Faculty of Physical Sciences  
Universidad Complutense de Madrid  
Pza. Ciencias 1, Ciudad Universitaria E-28040 Madrid, Spain  
E-mail: a.s.sanz@fis.ucm.es

**Abstract.** When teaching Optics, it is common to split up the formal analysis of diffraction according to two convenient approximations, in the near and far fields. Moreover, apart from a slight mention to the relationship between the wavelength and the typical size of the aperture that light is incident on, such analysis does not often involve any explicit mention to Geometrical Optics. By means of a simple laboratory demonstration, Panuski and Mungan have shown how the gradual variation of the width of a single slit leads to a smooth transition from the far field to the near field, eventually reaching what could be regarded as the Geometrical Optics limit for large enough openings. Here a simple pedagogical analysis of this transition is presented, which combines both analytical developments and numerical simulations, and is intended to serve as a guide to introduce in a more natural way (in positions, where real experiments take place) the above mentioned splitting taking as a reference such transition and its implications. In this regard, first this transition is investigated in the case of a Gaussian beam diffraction, since its full analyticity paves the way for a better understanding of the paradigmatic case of single-slit diffraction. Then, the latter case is then tackled both analytically, by means of some insightful approximations and guesses, and numerically, which explicitly shows the influence of the various parameters involved in diffraction processes, such as the typical size of the input (diffracted) wave or its wavelength, or the distance between the input and output planes. This analysis unveils staircase structures in the Fresnel regime, which seem to characterize the trend towards the Geometrical Optics limit in this case, against the smooth behaviors observed in the Fraunhofer regime.

## 1. Introduction

Due to the wave nature of light, and more specifically the phenomenon of diffraction, the intensity distribution observed behind a sharp opening is not homogeneous. Consider the paradigmatic case of a long rectangular slit [1, 2]. The intensity distribution generated by this slit exhibits a series of alternating maxima and minima aligned along the direction perpendicular to the long axis of the slit (i.e., the so-called transverse direction). As is well known and routinely taught in Optics courses [2], the phenomenon is observable whenever the wavelength of the incident light is comparable with the dimensions of the slit. Furthermore, it is also known [3] that, as the projection screen where the intensity is observed moves further away from the slit, the intensity

distribution gradually changes from a highly oscillatory pattern, at distances relatively close to the slit, to a stationary, scale invariant distribution, far enough from the slit. At the experimental level, a very detailed account on this continuous transition from the near field or Fresnel regime to the far field or Fraunhofer regime was reported by Harris *et al.* [4] in the late 1960s.

The different oscillatory behavior observed in the Fresnel and Fraunhofer regimes arises from the dependence of phase contributions in each case on the transverse coordinate in relation to the distance between the slit and the projection screen [1]. In the Fraunhofer regime, the linear dependence on this coordinate turns into a constant aspect ratio in relative terms, which explains the scale-invariance of the intensity pattern. On the contrary, in the Fresnel regime, a quadratic dependence produces fast phase variations from a distance to the next one, which translates, in turn, into a rapidly oscillatory pattern. This pattern, though, resembles the sharp shadow produced in the domain of geometrical optics, where the presence of the slit has no effect on the incident collimated ray bundle other than preventing the passage of rays incident beyond the slit boundaries. This effect becomes more apparent as the observation distance becomes closer and closer to the slit.

As it was shown by Panuski and Mungan [5], the above situation leads naturally to question oneself how the transition from wave optics (represented by Fraunhofer diffraction) to geometrical optics (somehow related to the first stages of a Fresnel regime) takes place, more specifically, whether there is a distinctive trait in such a transition that helps us to uniquely discriminate when we are in each regime (other than, of course, the semiquantitative, well-known Rayleigh criterion). Thus, following standard wave optics arguments [3], at a fixed distance,  $z$ , from the projection screen (and for monochromatic light), the width of the principal Fraunhofer diffraction maximum produced by a single slit shows a dependence with the inverse of the slit width, henceforth denoted by  $a$ . The width of this maximum thus falls as  $a$  increases. However, since  $z$  is kept constant, such increase also implies that the Fraunhofer condition is gradually lost; the Fresnel regime starts playing a role, in particular, making such falloff rate no longer valid. There is not a precise analytical way to determine the width of the main intensity maximum in the Fresnel regime in relation to  $a$ , because of the fast oscillations that the intensity distribution undergoes even with slight changes in  $a$ . Nonetheless, to some extent it roughly resembles a distribution more typical of geometrical optics, as mentioned above, with the shadow boundaries being determined by  $a$ . In other words, it is reasonable to assume that, for large enough values of  $a$ , the width of the main intensity maximum should increase linearly with  $a$ .

If those two arguments for the far and near fields must be satisfied, clearly the intensity distribution should present a turnover (minimum) as  $a$  is gradually increased, which is precisely the result experimentally reproduced by Panuski and Mungan [5]. More recently, in a further numerical analysis, Davidović and Božić showed [6] the nice agreement between the experimental data reported by Panuski and Mungan and the simple expression provided by the scalar theory of diffraction for single-slit diffraction in the paraxial approximation [2,3]. Typically, this transition from the Fresnel to the Fraunhofer regime is explained in the standard way, that is, appealing to the Fresnel linear-zone model and the concept of Cornu spiral [3]. This methodology has been rather convenient from an algebraic point of view to understand the diffraction phenomenon in the Fresnel regime, at least, when one tries to skip in as much as possible numerical computations. However, from an intuitive point of view,

simpler analytical comparative models can help the student to better understand such transition, particularly taking into account that it is a general trend, which does not depend on the specific transmission properties of the opening (although they might influence other aspects, such as the diffraction expansion rate or the overall profile displayed by the intensity distribution).

To better understand this transition, and more specifically the turnover when the slit width increases, in this work we first present an analytical study and discussion of the phenomenon in the case of Gaussian beam diffraction (which somehow mimics the behavior of a slit with a Gaussian transmission function). The simplicity of this fully analytic problem provides us with an intuitive first approach to the issue, where it is readily seen that any diffraction process can be split up into three different regimes depending on the expansion rate displayed by the diffracted beam, namely, Huygens, Fresnel and Fraunhofer, in agreement with the analysis presented in [6]. This is then applied to the case of the well-known single-slit diffraction, which is numerically investigated in terms of the quantity also considered by Panuski and Mungan, namely the full width at the 20% of the principal maximum (FW02M) in order to compare with the experimental data reported by these authors. It is seen that, when proceeding in a systematic way, while the dependence of the FW02M on  $a$  within the Fraunhofer regime is smooth, after crossing the turnover, a staircase structure characterizes the Fresnel regime, with shorter and shorter steps as  $a$  increases and the system gets into the Huygens (geometrical) regime.

The work is organized as follows. The analysis and discussion of Gaussian-beam diffraction is presented in Sec. 2. Section 3 is devoted to the diffraction by a long rectangular slit, first introducing a theoretical analysis and then the discussing a series of experimental results obtained with a simple arrangement (which is also described). To conclude, the main findings observed here and some remarks connected to their extrapolation to matter waves (where they should also be observable) are summarized in Sec. 4

## 2. Gaussian-slit diffraction

The Helmholtz equation in paraxial form is isomorphic to the time-dependent Schrödinger equation, with the longitudinal coordinate playing the role of the evolution parameter (the time in the Schrödinger equation) [7,8]. Accordingly, a Gaussian beam displays the same dispersion along the transverse direction than a quantum Gaussian wave packet does along time. Actually, both solutions can be exchanged if the factor  $\hbar t/m$  that rules the behavior of a quantum Gaussian wave packet is substituted by the factor  $z/k$  (or, equivalently,  $\lambda z/2\pi$ , with  $k = 2\pi/\lambda$ ), with  $z$  being chosen as the longitudinal coordinate [8]. A paradigmatic example of Gaussian diffraction is that of a single-mode laser beam released in free space.

Let us consider the electric field associated with such a laser beam [8],

$$\mathbf{E}(\mathbf{r}, z) = E_0 \frac{w_0}{w_z} e^{-r^2/w_z^2 - i(kz + kr^2/2R_z) + i\varphi_z} \hat{\mathbf{r}}, \quad (1)$$

where  $\mathbf{r}$  accounts for the radial (transverse) coordinate vector,  $w_0$  is the beam waist, and the other parameters are functions of the coordinate  $z$ , which accounts for the distance between the output (observation) and input (launch) planes (the latter is taken as the origin of the reference system). These  $z$ -dependent functions are the

width of the beam at the output plane,

$$w_z = w_0 \sqrt{1 + \frac{z^2}{z_R^2}}, \quad (2)$$

the radius of curvature of the beam at such a plane,

$$R_z = z \left( 1 + \frac{z^2}{z_R^2} \right), \quad (3)$$

and the Gouy phase,

$$\varphi_z = (\tan)^{-1} \left( \frac{z}{z_R} \right), \quad (4)$$

all of them given in terms of the Rayleigh range or distance,

$$z_R = \frac{kw_0^2}{2} = \frac{\pi w_0^2}{\lambda}. \quad (5)$$

Accordingly, the irradiance or intensity distribution at the output plane  $z$  is

$$I(r, z) = \frac{1}{2} \sqrt{\frac{\epsilon_0}{\mu_0}} |\mathbf{E}(\mathbf{r}, z)|^2 = \frac{1}{2} \sqrt{\frac{\epsilon_0}{\mu_0}} \frac{w_0^2}{w_z^2} e^{-2r^2/w_z^2}. \quad (6)$$

In this analysis the interest relies on the changes undergone by the intensity distribution as the output plane, so we will consider relative intensities, i.e.,

$$I_{\text{rel}}(r, z) = \frac{I(r, z)}{I(r=0, z)} = e^{-2r^2/w_z^2}. \quad (7)$$

Since the intensity (7) only depends on  $z$  through  $w_z$ , from now on let us focus on this parameter. Thus, by inspecting (2), three different stages or regimes in the propagation of the beam along the  $z$ -direction can be distinguished, each one characterized by specific features:

- The geometrical or Huygens regime, for  $z_R \gg z$ , where the beam does not exhibit any remarkable dispersion, but remains essentially with the same width, since  $w_z \approx w_0$ :

$$I_{\text{rel}}(r, z) \approx e^{-2r^2/w_0^2}. \quad (8)$$

In this regime, diffraction effects are negligible (Huygens principle applies in strict sense) and, therefore, the wavefronts are plane parallel ( $R_z \approx z_R^2/z \rightarrow \infty$ ). Thus, although diffractionless propagation is typically associated with the size of the wavelength, this case shows that the phenomenon also appears at the very early stages of the field propagation, in close analogy to the Ehrenfest regime in quantum mechanics [9]. Also note that the Gouy phase (4) can be neglected ( $\varphi_z \approx 0$ ) and hence it has no influence on the beam propagation.

- The far field or Fraunhofer regime, the opposite limit, for  $z_r \ll z$ , where the beam width increases linearly with the  $z$ -coordinate,  $w_z \approx w_0 z/z_R = \lambda z/\pi w_0^2$ , and the wavefronts are concentric, with their radius increasing linearly with  $z$  ( $R_z \approx z$ ). In this case, the relative intensity distribution remains invariant due to its dependence on the ratio  $x/z$ , i.e.,

$$I_{\text{rel}}(r, z) \approx e^{-2r^2 z^2 / w_0^2 z^2} = e^{-(2\pi w_0^2 / \lambda^2)(r/z)^2}. \quad (9)$$

In other words, the distance between two points in the distribution increases at the same rate independently of the distance  $z$  at which the distribution is observed. As it is inferred from (4), also here the phase remains essentially constant all the way down the evolution of the field, being  $\varphi_z \approx \pi/2$ .

- The near field or Fresnel regime, an intermediate range, where the curvature of the wavefronts is not well defined and the Gouy phase is a varying function of the  $z$ -coordinate, but still with a rather defining trait. Specifically, this regime is characterized by boosting the beam dispersion, that is, by provoking a fast increase of the beam width, from a nearly dispersionless behavior to an asymptotic linear increase. This regime is still around the range  $z_r \gg z$ , so that

$$w_z \approx w_0 \left( 1 + \frac{z^2}{z_R^2} \right), \quad (10)$$

which resembles to an accelerated term, since it depends quadratically on the propagation coordinate. Nonetheless, it is seen from (5) that the smaller the waist and the larger the wavelength, the shorter the Rayleigh range and the boost takes place at shorter distances. It can also be shown that local phase variations in (1) are actually ruled by a quadratic dependence on the transverse coordinates, unlike the Fraunhofer regime, where such dependence is linear.

Of course, the transition from negligible  $z$  to large  $z$  is continuous and there are intermediate regimes. Yet, these are essentially the three distinctive regimes that can be distinguished in any diffraction process regardless of the initial shape of the beam. Here, we have considered a Gaussian, but it can also be a constant amplitude function with a certain spatial extension, e.g., a sharp-edged slit receiving a constant illumination, as we will see in Sec. 3. These considerations are not only in agreement with the analysis and discussion presented in [6], in the context of the current experiment, but there is also a close connection with the spreading of Gaussian wave packets in quantum mechanics [9, 10].

The above discussed general features help us to understand how the width of a diffracted beam evolves as the beam propagates. Leaving aside the position of the output plane, the width of any beam essentially depends on both the wavelength  $\lambda$  of the incident radiation and the input width (the waist  $w_0$  at the input plane  $z = 0$ , in the case of the Gaussian beam), which can be related, in turn, to the size of the diffracting opening. These quantities have an influence on the beam diffraction, measurable in terms of the size of the beam at a given  $z$  and the relative intensity. Hence, to quantify the diffractive effect on the beam, we have considered the above mentioned full width at the 20% of the maximum, FW02M, which combines both physically measurable quantities. In the particular case we are dealing with here, namely that of a Gaussian beam, this value is simply given by the expression

$$\text{FW02M}(z; w_0, \lambda) = \sqrt{2 \ln 5} w_z = \sqrt{2 \ln 5} w_0 \sqrt{1 + \left( \frac{\lambda z}{\pi w_0^2} \right)^2}. \quad (11)$$

Note in this expression that the effect of increasing/decreasing  $\lambda$  or  $z$  is equivalent; in both cases, the trend is analogous to the one discussed above for  $z$  (in relation to  $z_R$ ), that is, the FW02M displays a hyperbolic dependence on the corresponding parameter (constant start and asymptotic linear increase, with an intermediate boost in between). If the input waist  $w_0$  is considered instead, a rather different behavior is observed on a projection screen at a given output distance  $z$  (and an also fixed  $\lambda$ ):

- For  $w_0 \ll \sqrt{\lambda d / \pi}$ , i.e., for a relatively narrow input Gaussian beam, the width of the observed intensity distribution decreases with  $w_0$ ,

$$\text{FW02M} \approx \sqrt{2 \ln 5} \frac{\lambda z}{\pi w_0}, \quad (12)$$

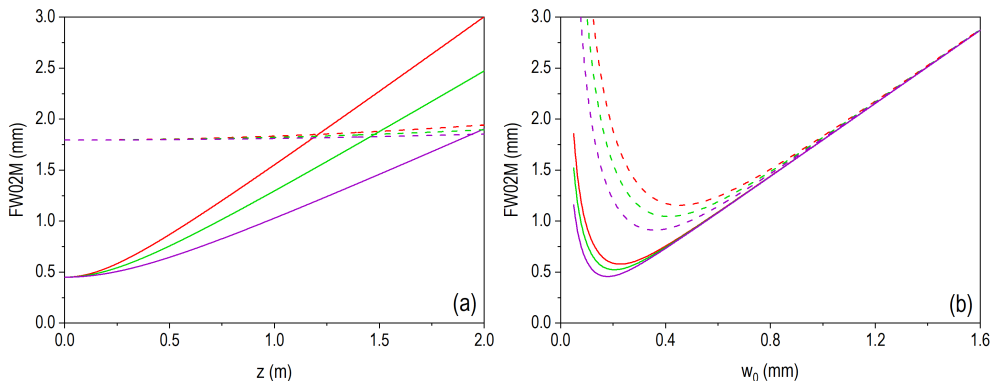


**Figure 1.** Full width at 20% the maximum intensity (FW02M) for a diffracted Gaussian beam in terms of its distance between the input and output planes (a) and the size of its waist (b) for three different values of the wavelength:  $\lambda = 650$  nm (red),  $\lambda = 532$  nm (green), and  $\lambda = 405$  nm (violet). To compare with, in panel (a) two input waist sizes are considered:  $w_0 = 0.25$  mm (solid line) and  $w_0 = 1$  mm (dashed line). Similarly, in panel (b) two distances are considered:  $z = 0.25$  m (solid line) and  $z = 1$  m (dashed line).

as one would expect from a typical Fraunhofer regime. In other words, this result indicates that  $z$  has been chosen in such a way that the intensity distribution is well inside the Fraunhofer regime.

- For  $w_0 \gg \sqrt{\lambda z/\pi}$ , i.e., for a relatively wide input Gaussian beam, the width of the observed intensity distribution increases linearly with  $w_0$ ,

$$\text{FW02M} \approx \sqrt{2 \ln 5} w_0. \quad (13)$$

This result is in correspondence with a geometrical regime, where the effective extension of the irradiance distribution at the output plane  $z$  is proportional to its extension at the input plane.

In sum, we find a clear transition from a fully diffractive (Fraunhofer) regime to a seemingly geometrical one, each one with a very specific dependence on  $w_0$ . Hence, at some point, there should be a turnover. Getting back to Eq. (11), for fixed  $\lambda$  and  $z$ , we find that it has a minimum when the input waist  $w_0$  reaches the critical value

$$w_c = \sqrt{\frac{\lambda d}{\pi}}. \quad (14)$$

Substituting this value into Eq. (11) leads to the FW02M turnover value,

$$\text{FW02M}_t = 2\sqrt{\ln 5} w_c = 2\sqrt{\ln 5} \sqrt{\frac{\lambda d}{\pi}} \approx 1.4315\sqrt{\lambda d}. \quad (15)$$

To better appreciate these facts, the FW02M (11) is displayed in Fig. 1, where realistic values, which can easily be reproduced in any teaching laboratory, have been assigned to the different parameters involved in the calculations. Thus, the three wavelengths considered correspond to standard laser pointers,  $\lambda = 650$  nm,  $\lambda = 532$  nm, and  $\lambda = 405$  nm, with maximum output power below 5 mW and uncertainties of the order of  $\pm 10$  nm, but that basically cover the visible spectral range (very appropriate to conduct the experience in the laboratory with students). The dependence of the FW02M on the distance between the input and output planes,

$z$ , is shown in Fig. 1(a) for two values of the input waist,  $w_0 = 0.25$  mm (solid lines) and  $w_0 = 1$  mm (dashed lines), and the above three wavelengths (each curve with the corresponding color: red, green, and violet). As it can be noticed, the wider the Gaussian beam at the input plane the lesser its spreading at the output plane, which implies an also lesser difference among the three wavelengths. Furthermore, it is also clearly seen that, as the beam size decreases, the three expansion regimes (Huygens, Fresnel, and Fraunhofer) of the beam are more clearly observable. See, for instance, the case for  $w_0 = 0.25$  mm, where the FW02M remains basically constant up to  $z \approx 0.05$  m, then it undergoes a nearly quadratic (hyperbolic) increase up to  $z \approx 0.3$  m, and finally it exhibits a linear increase regardless of the value of  $z$ . In the case of the wider beam ( $w_0 = 1$  mm), on the contrary, the linear regime is not reached within the range of 2 m here considered. Note that, if we consider an average wavelength  $\bar{\lambda} = 529$  nm, the Rayleigh range corresponding to  $w_0 = 0.25$  mm is  $\bar{z}_R = 0.37$  m, while for  $w_0 = 1$  m we have  $\bar{z}_R = 5.94$  m, both in agreement with the values inferred from the numerical simulations. Yet, the gradual increase observed with  $z$  does not allow us to set a clear distinction between the Fraunhofer and the geometrical regimes. The same happens if instead of varying  $z$  we would have chosen varying  $\lambda$ , according to Eq. (11).

To that end, let us now consider the dependence of the FW02M on the input waist  $w_0$ , which is represented in Fig. 1(b) for the same wavelengths (same color code) and two different distances between the input and output planes  $z$ , namely,  $z = 0.25$  m (solid lines) and  $z = 1$  m (dashed lines). The picture that emerges now is quite different, with two well-defined trends for the two distances and all wavelengths, one of them falling down with  $w_0$ , in agreement with Eq. (12), and another linearly increasing with  $w_0$ , as indicated by Eq. (13). Furthermore, it is also clearly seen how an increase in the wavelength or in the distance to the output plane produce an increase in the position of the transition input waist  $w_c$ , in compliance with the fact that an increment in any of these quantities (or both) allows us to observe a wave behavior (Fraunhofer diffraction features) with wider and wider input beams. This implies the observation of increasingly wide diffraction maxima, i.e., larger values of the FW02M. In turn, this also implies that, to observe geometrical type features, the width of the input beam must be larger. However, following Eq. (13), the FW02M does not experience any difference and tends to converge to the values for any other  $\lambda$  and/or  $z$ , since it only depends on  $w_0$ , as it is expected in a typically geometrical regime. Of course, the transition threshold also undergoes a displacement towards larger values of the input waist. With the values here considered, for the same wavelength, this displacement doubles when the projection screen is moved from  $z = 0.25$  m to  $z = 1$  m.

Before concluding this section, we would like to briefly mention that the general shape displayed by the graphs in Fig. 1(b), and particularly the presence of a turnover that separates two physically different trends or behaviors, to some extent resembles a result found in quantum gravity, for micro-black holes, in the context of the so-called generalized uncertainty principle [11]. Within this scenario, the quantity that plays the role of the critical beam width  $w_0$  is the Planck energy, observing a similar trend between a given space region of a certain width and the energy that it contains. If quantum fluctuations are important, then there is an inverse relation between the two quantities; if classical gravitation is relevant, then they are proportional. The critical length at which these two behaviors coincide is precisely the Planck length (for energy uncertainties of the order of the Planck energy), at which a micro black hole could originate.

### 3. Diffraction by a long rectangular slit

#### 3.1. Theoretical analysis

Let us now consider the diffraction through a very long rectangular slit, with the  $x$ -axis in the direction of the shorter side, with length  $a$ , and the  $y$ -axis along the longer one, with length  $b \gg a$ . Due to translation symmetry along the  $y$ -direction, the problem can be solved and explained, in a good approximation, within the  $XZ$ -plane, where  $x$  will denote the transverse coordinate and  $z$  the longitudinal (propagation) one. Appealing again to paraxial conditions, the electric field amplitude solution to the (paraxial) Helmholtz equation can be recast [1] as

$$E(x, z) \propto E_0 \int_{-a/2}^{a/2} e^{i\pi(x-x')^2/\lambda z} dx', \quad (16)$$

in the case of an incident field with constant amplitude within the opening determined by the slit, from  $-a/2$  to  $a/2$ , and where prefactors and global phase factors are neglected for simplicity, but without any loss of generality (a detailed derivation of the general paraxial solution can be found in [12] in the context of matter waves and the Schrödinger equation). Note in (16) that, if the output plane  $z$  is fixed, the expression can be rewritten as

$$E(x, z) \propto E_0 \int_{-a/2}^{a/2} e^{i(x-x')^2/w_c^2} dx', \quad (17)$$

where  $w_c$  is given by Eq. (14), although this parameter now is regarded as a generalized typical distance to compare with, instead of referring to the particular case of the waist of a Gaussian beam.

As in Sec. 2, here we also consider the relative intensity distribution,

$$I_{\text{rel}}(x, z) = \frac{I^2(x, z)}{I^2(x=0, z)} \propto \left| \int_{-a/2}^{a/2} e^{i(x-x')^2/w_c^2} dx' \right|^2, \quad (18)$$

where  $I(x, z) \propto |E(x, z)|^2$ ,  $x'$  and  $x$  describe positions on the input and output plane, respectively (which correspond to the planes where the slit and the projection screen are accommodated). In principle, the next step in the analysis would consist, also as in Sec. 2, in investigating the behavior of (18) and determining the different propagation regimes. However, this task is not that simple for the intermediate stages, e.g., the Fresnel regime, which requires the use of numerical techniques. Yet, the integral is simple enough to allow us extracting some physics leaving aside further calculations (although, in the end, they are necessary to determine and understand the full trend), which is quite beneficial at a pedagogical level. Thus, let us first focus on the integral, which can be conveniently recast as

$$\mathcal{I}(x, z) = \int_{-a/2}^{a/2} e^{i(x'^2 - 2xx')/w_c^2} dx', \quad (19)$$

where the factor  $e^{ix^2/w_c^2}$  has been removed without any loss of generality, since it is automatically suppressed in (18) and hence has no physical relevance at all here. In order to make apparent the three regimes described in Sec. 2, the question to be addressed now is whether, for a given  $z$  (or, in general, a given value of the typical length scale  $w_c$ ), the phase terms  $x'^2$  and  $2xx'$  are relevant, and, if so, which one dominates. When proceeding this way, the following scenarios readily arise for a given wavelength of interest:

- If  $z \approx 0$ , the integrand becomes a very rapidly oscillatory function. On average, one could then assume that only when the function is evaluated over the actual point  $x$  [i.e.,  $x' \approx x$  in the integrand of Eq. (18)], there is a non-vanishing contribution. If this is extended to the full integration range, in a good approximation the result of the integral (19) is a constant, namely,  $\mathcal{I}(x, z) \approx a$ . This corresponds to a geometrical regime, where there is a nearly constant irradiance in front of the slit, surrounded on either side by a region of geometrical shadow. This thus corresponds to the Huygens regime, ruled out by geometrical optics, which holds for either small distances between input and output planes, but also, if  $z$  is fixed, for negligible wavelengths, as it is typically taught.
- For longer but small enough values of  $z$ , so that the values  $x$  of interest (where the intensity is important) are still within the  $(-a/2, a/2)$  interval or nearby, the trend is similar, although the phase terms start playing a role, particularly, the  $x'^2$  term, which is typically smaller and hence leads to important oscillations. This quadratic dependence on the slit coordinate is typical of the Fresnel regime and physically manifests as the appearance of rather prominent oscillations in the intensity distribution, with some leaks towards the geometrical shadow region, even though it still mainly concentrates within the area covered by the slit. Note that, if the second phase term is neglected in Eq. (19), the Fresnel integrals readily appear, which leads to the usual methods in wave optics developed to determine analytically the on-axis intensity (Fresnel zones and the Cornu spiral).
- Finally, at rather long values of  $z$ , far beyond the slit input plane, it is the second phase term the one that becomes prominent, since  $x$  may acquire values beyond the interval  $(-a/2, a/2)$ . In this case, the integral (19) has a simple analytical solution:

$$\mathcal{I}(x, z) \sim \int_{-a/2}^{a/2} e^{-2ixx'/w_c^2} dx' \propto \text{sinc}\left(\frac{\pi ax}{\lambda z}\right). \quad (20)$$

With this, the intensity (18) becomes

$$I_{\text{rel}}(x, z) = \text{sinc}^2\left(\frac{\pi ax}{\lambda z}\right), \quad (21)$$

which is the typical intensity distribution generated by a single slit in the Fraunhofer regime. The profile displayed by this intensity distribution at the output plane regardless of the value of  $z$ ; it only depends on the ratio  $x/z$ , which determines the observation angle,  $\theta \approx x/z$ , in paraxial approximation.

We thus see in a simple and intuitive manner that, effectively, the three regimes are a general trait of any diffraction process, independently of the shape of the initially diffracted field (the field at the input plane).

Let us now get back to the question of determining the width of the intensity distribution at a fixed output plane  $z$ , also measured in terms of the FW02M. From the above discussion, and following the reasoning given by Panuski and Mungan, a suitable guess in the geometrical regime for the FW02M is

$$\text{FW02M} \propto a, \quad (22)$$

assuming that Fresnel diffraction features are negligible, at least, at first approximation. Of course, some deviations should be expected, but in the limit a very large slit width, the approximation should be good enough. On the contrary, for tiny slit widths, one should expect Fraunhofer diffraction to be dominant and a

decreasing trend for FW02M with increasing  $a$ , as it is inferred from Eq. (21). In order to determine an analytical expression for the FW02M in this case, let us consider the sine approximation formula developed by the VIIth-century Indian astronomer and mathematician Bhaskara I [13],

$$\sin u \approx \frac{16u(\pi - u)}{5\pi^2 - 4u(\pi - u)}, \quad (23)$$

where  $u$  is measured in radians ( $0 \leq u \leq \pi$ ). From this formula, it follows that the sinc-function can be approximated as

$$\text{sinc } u \approx \frac{16(\pi - u)}{5\pi^2 - 4u(\pi - u)}. \quad (24)$$

In our case, in particular, we have  $u = \pi ax/\lambda z$ . If we search for the value of  $u$ , such that  $\text{sinc}^2 u = \beta^2$ , we find

$$u = \frac{1}{2} \left( \pi - \frac{4}{\beta} + \frac{2}{\beta} \sqrt{4 + 2\pi\beta - \pi^2\beta^2} \right). \quad (25)$$

After substituting  $\beta = \sqrt{0.2} = 1/\sqrt{5}$  into this latter expression, we find

$$u = \frac{\pi}{2} - 2\sqrt{5} + \sqrt{20 - \pi^2 + 2\pi\sqrt{5}} \approx 2.01598 \quad (26)$$

(the negative root is neglected, because of the domain of definition for  $u$  indicated above). Therefore, the expression of the FW02M in the Fraunhofer regime reads as

$$\text{FW02M} \approx \frac{2u\lambda z}{\pi a} \approx 1.28341 \frac{\lambda z}{a}, \quad (27)$$

which shows the expected dependence on the inverse of the slit width  $a$ . Since there is no an analytical expression for the FW02M that covers the full range of slit widths, as in the case of the Gaussian beam, in order to determine in an approximate manner the critical width  $a_c$ , we use the guess that, for this value, Eqs. (22) and (27) should equal. This renders a critical slit-width value

$$a_c \approx 1.13288 \sqrt{\lambda z} \approx 2.00797 \sqrt{\frac{\lambda z}{\pi}}. \quad (28)$$

If this value is substituted into Eq. (27), we obtain the approximated value for the turnover FW02M,

$$\text{FW02M}_t \approx 1.13287 \sqrt{\lambda z} \approx 2.007966 \sqrt{\frac{\lambda z}{\pi}}, \quad (29)$$

which is about twice the turnover value found for the Gaussian beam.

Of course, the above conclusions are just feasible analytical conjectures, which do not provide further details about the transition that we studying here, and, moreover, must also be somehow tested. Hence, in order to get a deeper understanding of the problem, next two intertwined routes are considered, namely, a numerical analysis, which renders some light on the trends analytically found, as it was done in the case of Gaussian beams, and a comparison with the experiment, with the purpose to verify the validity of such numerical analysis.

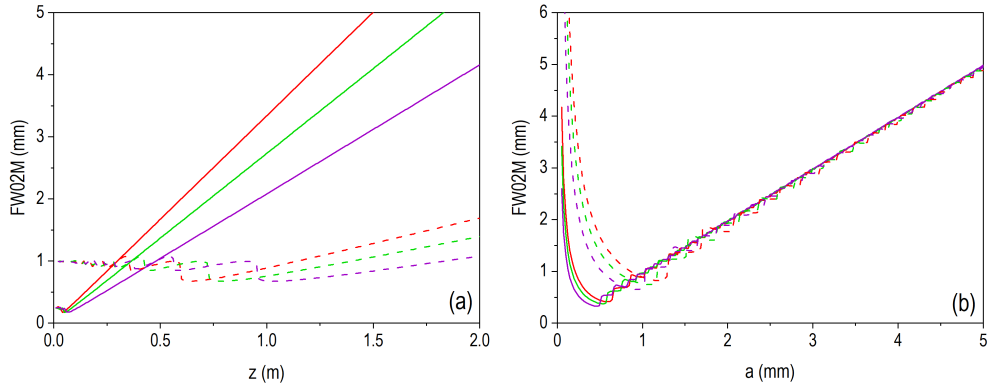


**Figure 2.** Full width at 20% the maximum intensity (FW02M) for the diffraction of a monochromatic plane waves incident on a very long rectangular slit in terms of the distance between the input and output planes  $z$  (a) and the slit width  $a$  (b) for three different values of the wavelength:  $\lambda = 650$  nm (red),  $\lambda = 532$  nm (green) and  $\lambda = 405$  nm (violet). To compare with, in panel (a) two slit widths are considered:  $a = 0.25$  mm (solid line) and  $a = 1$  mm (dashed line). Similarly, in panel (b) two distances are considered:  $z = 0.25$  m (solid line) and  $z = 1$  m (dashed line).

### 3.2. Numerical analysis

As in Sec. 2, in Fig. 2 we show the dependence of the FW02M on the distance between the input and output planes (a), and on the slit width  $a$  (b), which is the analog to the Gaussian beam waist  $w_0$ . In each case, the same three wavelengths have been considered. More specifically, the FW02M is automatically determined with the aid of a simple on-purpose built numerical Fortran-based code, which computes the relative intensity distribution (18), normalizes its maximum to unity, and then finds the  $x$ -positions ( $x_1$  and  $x_2$ , symmetrically distributed around  $x = 0$ ) at which the latter equals 0.2 in order to determine the FW02M (with  $\text{FW02M} = x_2 - x_1$ ). Proceeding this way, we have thus obtained the results shown in Fig. 2(a) for two slit widths:  $a = 0.25$  mm (solid lines) and  $a = 1$  mm (dashed lines). Consider the case for the smallest slit width. Unlike the smooth dependence exhibited by the Gaussian beam, it is observed that there is a very short Huygens regime, followed by a jump-type structure characterizing the intermediate Fresnel regime, and, immediately after, the Fraunhofer regime starts, which is clearly determined by a distinctive linear trend. If the slit width increases, the same behavior is observed, although the distance  $z$  at which the Fraunhofer regime is reached increases very rapidly. Note that, on average, an increase from 0.25 mm to 1 mm in  $a$  implies an increase from  $\sim 0.05$  mm to  $\sim 1$  mm. Although the near field structure is more complex than the same region for the Gaussian beam, we find again the same lack: it is difficult to observe the transition we are investigating, because we cannot see a clear turnover.

To mitigate that problem, we proceed as before and compute the FW02M against the slit width, which is shown in Fig. 2(b) for the same three wavelengths and two values of the distance between the input and output planes:  $z = 0.25$  m (solid lines) and  $z = 1$  m (dashed lines). Thus, the numerical simulations render two important general trends. First, an initial falloff with increasing (but small values of)  $a$ , which is in compliance with the behavior described by Eq. (27), i.e., with the inverse of the

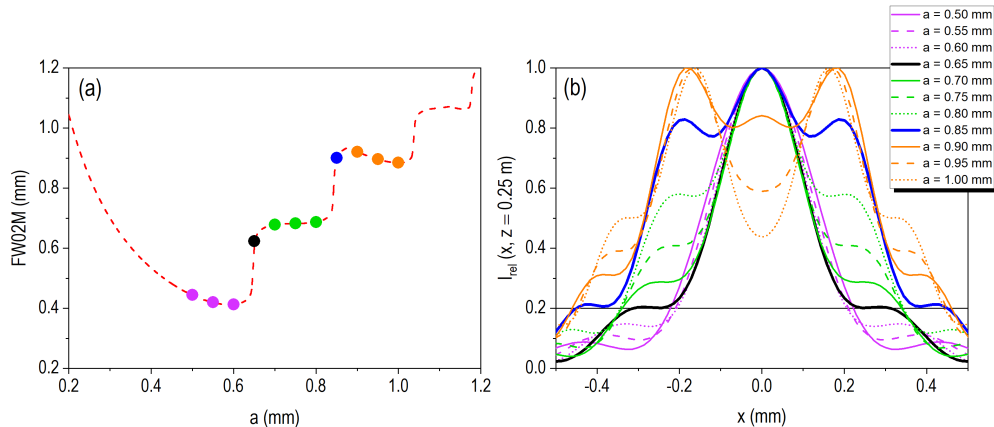


**Figure 3.** (a) Detail of the full width at 20% the maximum intensity (FW02M) displayed in Fig. 2 for  $\lambda = 650$  nm and  $z = 0.25$  m. Solid circles denote the sampling values considered to analyze the staircase structure displayed by the FW02M around the turnover region. (b) Relative intensity distributions (at  $z = 0.25$  m) associated with the selected values of slit widths shown in panel (a). Same color line (but different type) is used for values on the same step; thicker lines correspond to values at the jump.

slit width. Second, an incipient overall linear trend is observed for large values of  $a$ , which is in correspondence with the guess (22). Furthermore, we also find that there is a turnover denoted by the presence of a minimum in the representation, as in the case of the Gaussian beam [see Fig. 1(b)], which more or less coincide with the values estimated above,  $a_c$  and  $\text{FW02M}_t$ . For instance, if we consider the average wavelength  $\bar{\lambda} = 529$  nm, the turnover is obtained at  $a_c \approx 0.4$  mm for  $z = 0.25$  m, and at  $a_c \approx 0.8$  for  $z = 1$  m, which coincides with what we observe in Fig. 2(b). In either case, though, these values are larger than for a Gaussian beam, because the expansion of “top-hat” type diffracted beams is typically faster, which requires larger openings to observe slower diffractive rates. Anyway, it seems that the preliminary analytical treatment, based on a series of reasonable work hypotheses, is not that bad. However, what such analytical treatment does not describe is the presence of the staircase structure that starts at the transition between the end of the Fraunhofer regime and the beginning of the Fresnel one, and somehow influences the turnover region, avoiding us to clearly identify a valid minimum (note that the minimum observable now is affected by such staircase structure). Yet the extrapolation of a linear regression at large values of  $a$ , where the steps become smaller and smaller, allows us to determine the turnover from the intersection between this linear fitting and the Fraunhofer falloffs, which render basically the estimated values mentioned before.

The staircase structure of Fig. 2(b) is connected to the systematic method employed by our numerical code, which determines the precise value where the relative intensity reaches the 20% of its maximum value. To determine the origin of this structure, absent in the case of Gaussian beams, let us focus on an enlargement of Fig. 2(b) around the turnover region, displayed in Fig. 3(a). In the latter figure, the turnover region is seen for a wavelength  $\lambda = 650$  nm and a distance  $z = 0.25$  m. The numerical simulation is denoted with the black solid line. Some sampling values associated with different slit widths are also shown (red and blue solid circles), which

cover three step levels and will be used to elucidate the emergence of this slit (in particular, the blue circles are markers associated with the border between one step and the next one). The profiles of the relative intensities related to each one of those markers are represented in Fig. 3(b) with different colors, which cover slit widths ranging from 0.5 mm to 1 mm, in tiny increments of 0.05 mm. As it can be noticed, because the turnover region is fully immersed in the Fresnel regime (actually, for moderate values of  $a$ , we should talk about the intermediate regime between the Fraunhofer and Fresnel ones [3]), such small increments may induce important changes, as it is seen near the sudden jumps from one step to the next one. What happens is that the intensity is characterized by marginal oscillating “wings”, as seen in Fig. 3(b), which start developing as the Fraunhofer regime blurs, and diffraction minima no longer vanish, particularly those adjacent to the principal maximum. The general behavior of these minima is that they start increasing, progressively elevating with them the secondary maxima and generating a highly wavy intensity distribution as  $a$  increases. Each time that the one of these secondary maxima reaches the 20% intensity threshold, we observe a sudden increase of the width (i.e., the FW02M). For example in Fig. 3(b), this is seen to happen for  $a = 0.65$  mm (green thick solid line) and  $a = 0.85$  mm (black thick solid line); in the first case, the jump is associated with the disappearance of the first adjacent secondary maxima, while in the second case the jump is connected to the second adjacent secondary maxima. Note that, eventually, the intensity pattern displays the well-known profile of a nearly flat distribution, more or less along the length extension covered by the slit, modulated by a series of small-amplitude and rapidly-varying oscillations both at the top and also at the sides, in the regions of geometrical shadow. This is the behavior typically considered in textbooks to illustrate the Fresnel regime [1–3], and where the plot in Fig. 2(b) exhibits a nearly linear trend for large  $a$ .

### 3.3. Comparison with the experiment

In order to test the validity of the approach that we have followed here, we have considered a comparison with the experimental data reported by Panuski and Mungan [5], which supplement the theoretical work recently published by Davidović and Božić [6] based on a conventional approach of considering the variation of the intensity distribution in terms of the Fresnel number (zones),  $FN = a^2/4\lambda z$ . Thus, in Fig. 4 we show the numerical FW02M as a function of the slit width obtained with the experimental parameters provided in [5], namely  $\lambda_{\text{exp}} = 660$  nm and  $z_{\text{exp}} = 0.656$  m. As it is seen, it exhibits the typical staircase structure beyond the turnover region, which gradually approaches a nearly linear tail for large  $a$ . The experimental data (solid circles) are superimposed to it in order to observe the good agreement with the theoretical (numerical) trend. The staircase structure, though, is not observed. After closely inspecting and analyzing the experimental data, particularly observing the slight discrepancies between the theoretical and experimental intensity distributions (some of which are represented in the insets for the slit widths indicated), we come to the conclusion that, in order to observe the staircase structure, the quality of the data recording requires some further refinement, for small fluctuations around the sudden jumps will suppress the effect. Nonetheless, getting back to the experimental data shown in Fig. 4, we find that the turnover region is around the critical value that we directly obtain from Eq. (28) for  $\lambda_{\text{exp}}$  and  $z_{\text{exp}}$ , namely,  $a_c \approx 0.74$  mm, which is closer to the experimental turnover than the former estimate,  $a_c \approx 0.931$  mm, provided

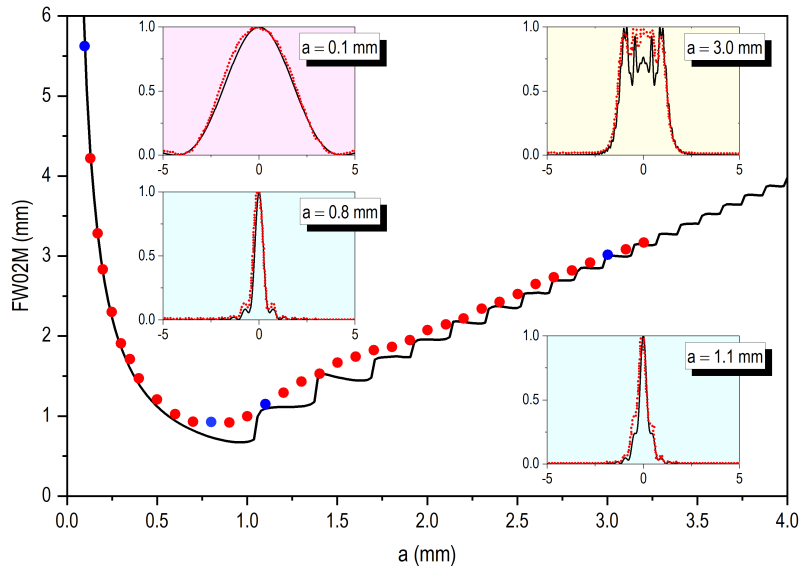


**Figure 4.** Comparison with the experimental data reported by Panuski and Mungan [5], with  $\lambda_{\text{exp}} = 660$  nm and  $z_{\text{exp}} = 0.656$  m. In the main panel, the experimental data are denoted by solid circles, while the theoretical simulation following Eq. (18) is described by the black solid line. In the insets, relative intensity for four different values of the slit width  $a$ :  $a = 0.1$  mm,  $a = 0.8$  mm,  $a = 1.1$  mm, and  $a = 3.0$  mm. Again here the red solid circles refer to experimental data, while the solid line indicates the intensity rendered by the theoretical model, Eq. (18). These four particular cases are denoted in the main panel with blue solid circles and have been picked up in different regimes, two in the limiting cases (Fraunhofer and geometrical regimes) and two in the turnover region.

in [5].

#### 4. Final remarks

In this work, an analysis of the transition from the Fraunhofer diffractive regime to the geometrical optics limit has been carried out with the purpose to better understand the meeting point between wave optics and geometrical optics, an aspect that is typically regarded with the size of the wavelength in textbooks. It is clear that, if the wave optics is regarded as a correct theory in all wavelength regimes, a smooth transition should be observable towards the domain of the geometrical optics, which is just a ray-based approximation. Moved by the experiments carried out by Panuski and Mungan [5], which show how this transition takes place in a nice manner, beyond wavelength considerations, here we have tackled the issue by first investigating the behavior of Gaussian beams and then the case of single slit diffraction. In both cases it is seen how, by means of a full analytical treatment, we have shown that when the width of the intensity is analyzed in terms of the beam or slit size, a turnover critical value for this size readily arises, which depends on only two parameters, namely, the wavelength  $\lambda$  of the monochromatic source considered, and the distance  $z$  between the input (slit) and output (projection screen) planes. Analytical expressions have been found for the critical values in both cases, which are proportional to  $\sqrt{\lambda z}$ . Accordingly,

it is seen that the rapid falloff with the inverse of the slit width, which characterizes the width of the intensity distribution in the Fraunhofer regime, gives rise to a linearly increasing width of the distribution beyond the critical slit width, in correspondence with the expectations from a geometrical optics perspective. For a comparison with the experimental data, the full width at a 20% of the principal maximum, FW02M, has been considered in the two cases to study these trends. We have seen that the turnover minimum is also in good agreement with the value determined from our analysis.

Furthermore, the theoretical analysis has also been followed by a numerical analysis in order to further investigate the trend displayed in the case of single-slit diffraction as well as the suitability of the approximations considered in the theoretical study. The simulations have shown that, while the Fraunhofer falloff is clearly seen, the transition towards the geometrical regime goes through a staircase structure with shorter and shorter steps, which starts in the turnover region. This structure is directly related to the gradual suppression of the typical Fraunhofer diffraction pattern, where each jump in the staircase corresponds to a sort of quantized increase of the FW02M coming from the adjacent secondary maxima. Although the experimental data reported in [5] do not allow to perceive this structure, they fit pretty well the asymptotic behavior towards the geometrical regime.

To conclude, it is worth mentioning that the treatments and findings account for here can be straightforwardly extended to matter waves. As it was mentioned above, in Sec. 2, the isomorphism between the paraxial Helmholtz equation and the time-dependent Schrödinger equation enables a direct translation of the findings reported here to matter waves, which, in principle, should be observable with the appropriate experimental conditions. Since fundamental aspects of interference have been explored with electrons [14,15] and large molecular complexes [16–18], these systems could also be used to investigate the behaviors here observed.

## References

- [1] Born M and Wolf E 1999 *Principles of Optics. Electromagnetic Theory of Propagation, Interference and Diffraction of Light* 7th ed (Cambridge: Cambridge University Press)
- [2] Hecht E 2002 *Optics* 4th ed (New York: Addison-Wesley Longman)
- [3] Elmore W C and Heald M A 1969 *Physics of Waves* (New York: McGraw-Hill)
- [4] F S Harris J, Tavenner M S and Mitchell R L 1969 *J. Opt. Soc. Am.* **59** 293–296
- [5] Panuski C L and Mungan C E 2016 *Phys. Teacher* **54** 356–359
- [6] Davidović M D and Božić M 2019 *Phys. Teacher* **57** 176–178
- [7] Sanz A S and Miret-Artés S 2012 *A Trajectory Description of Quantum Processes. I. Fundamentals (Lecture Notes in Physics vol 850)* (Berlin: Springer)
- [8] Sanz A S, Davidović M and Božić M 2020 *Appl. Sci.* **10** 1808(1–25)
- [9] Sanz A S and Miret-Artés S 2012 *Am. J. Phys.* **80** 525–533
- [10] Sanz A S 2012 *J. Phys.: Conf. Ser.* **361** 012016(1–11)
- [11] Scardigli F 199 *Phys. Lett. B* **452** 39–44
- [12] Sanz A S, Davidović M and Božić M 2015 *Ann. Phys.* **353** 205–221
- [13] Shirali S A 2011 *Math. Mag.* **84** 98–107
- [14] Bach R, Pope D, Liou S H and Batelaan H 2013 *New J. Phys.* **15** 033018(1–7)
- [15] Beierle P J, Zhang L and Batelaan H 2018 *New J. Phys.* **20** 113030(1–12)
- [16] Arndt M, Nairz O, Vos-Andreae J, Keller C, van der Zouw G and Zeilinger A 1999 *Nature* **401** 680–682
- [17] Gerlich S, Eibenberger S, Tomandl M, Nimmrichter S, Hornberger K, Fagan P J, Tüxen J, Mayor M and Arndt M 2011 *Nat. Commun.* **2:263** 1–5
- [18] Juffmann T, Milic A, Müllneritsch M, Asenbaum P, Tsukernik A, Tüxen J, Mayor M, Cheshnovsky O and Arndt M 2012 *Nat. Nanotech.* **7** 297–300